

Statistically Representative Three-Dimensional Microstructures for Modeling Microstructural Evolution in Aluminum

Abhijit Brahme¹, David M. Saylor², Joseph Fridy³, Anthony D. Rollett¹

1. Department of Material Science and Engineering, Carnegie Mellon University,

2. National Institute of Standards and Technology, Gaithersburg, MD, 20899, USA

3. Alcoa Technical Center, Alcoa Center, PA, 15069, USA

Abstract

Geometric and crystallographic observations from two orthogonal sections through a polycrystal were used as an input to the computer simulations to create a statistically representative three dimensional model. The microstructure is generated using a voxel-based tessellation technique. Assignment of orientations to the grains is done such that nearest neighbor relationships match the observed distributions. The microstructures thus obtained are allowed to evolve using a Monte-Carlo simulation. Anisotropic grain boundary properties are used in the simulations. Texture changes were observed during recrystallization in both experiments and in the corresponding simulations. Preliminary results demonstrate that the final texture has a strong dependence upon the nucleation scheme discussed in the paper. The good agreement between experiment and simulation obtained suggests that the assumptions about grain boundary anisotropy and nucleus placement were reasonable.

Introduction

In the present paper, methods are described to create statistically relevant three-dimensional model microstructures from spatially resolved orientation measurements on orthogonal section planes and to simulate the subsequent evolution of the microstructure during recrystallization. The objective of the work is to devise a model of microstructural evolution that is validated by direct comparison to experimental recrystallization data and will therefore have predictive capability. The methods are demonstrated using data collected from a rolled polycrystalline aluminum sample. The representation of the grain geometries is obtained in terms of a distribution of ellipsoids. The microstructure crystallography is described by assignment of orientations to the grains in the geometrically representative microstructure. Monte-Carlo simulations are subsequently performed for simulation of grain growth and recrystallization. The effect of different nucleation schemes on texture evolution is investigated. Significant growth of the cube component, $\{001\}\langle 100 \rangle$ is observed which appears to be dependent on

both the grain boundary anisotropy and on the heterogeneous spatial distribution of nuclei.

Observations from polycrystalline aluminum are used generating microstructural models. Orientation maps were obtained on two orthogonal observation planes using electron back scattering diffraction (EBSD). These are used as inputs the microstructure builder. Figure 1 shows the experimental geometry arranged such that the sample axis e_1 is aligned parallel to the rolling direction, sample axis e_2 is parallel to the transverse direction and the sample axis e_3 is parallel to the normal direction.

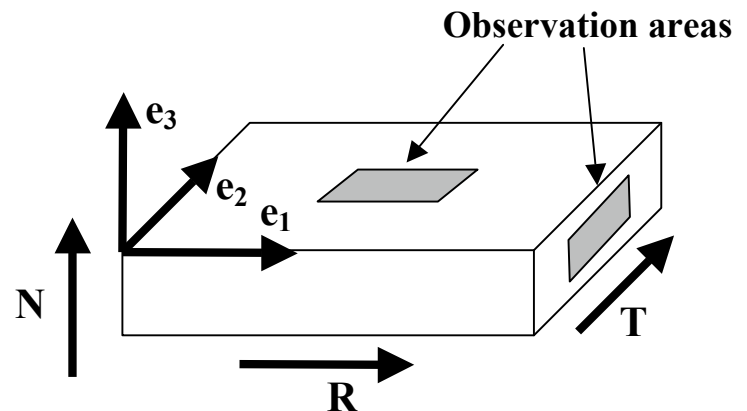


Figure 1: Schematic representation of experimental geometry.

Microstructure Generation

Ellipsoid Distribution:

A distribution of ellipsoids was used to represent grains in the polycrystalline microstructure that describe both the variations in grain size and aspect ratio. The main assumption here is that every grain can be approximated by ellipsoids. This assumption is justified by the geometry of the observed grains in the polycrystalline aluminum material. In addition to this, two more assumptions are made. The first one is that the distribution of ellipsoids is independent of position in the sample. That is there is no gradient in the grain size or morphology through the sample. Second assumption is that there is no variation in the orientation of the ellipsoids. Thus, to represent the distribution of grain sizes and

Report Documentation Page				Form Approved OMB No. 0704-0188	
Public reporting burden for the collection of information is estimated to average 1 hour per response, including the time for reviewing instructions, searching existing data sources, gathering and maintaining the data needed, and completing and reviewing the collection of information. Send comments regarding this burden estimate or any other aspect of this collection of information, including suggestions for reducing this burden, to Washington Headquarters Services, Directorate for Information Operations and Reports, 1215 Jefferson Davis Highway, Suite 1204, Arlington VA 22202-4302. Respondents should be aware that notwithstanding any other provision of law, no person shall be subject to a penalty for failing to comply with a collection of information if it does not display a currently valid OMB control number.					
1. REPORT DATE 2003		2. REPORT TYPE		3. DATES COVERED 00-00-2003 to 00-00-2003	
4. TITLE AND SUBTITLE Statistically Representative Three-Dimensional Microstructures for Modeling Microstructural Evolution in Aluminum				5a. CONTRACT NUMBER	
				5b. GRANT NUMBER	
				5c. PROGRAM ELEMENT NUMBER	
6. AUTHOR(S)				5d. PROJECT NUMBER	
				5e. TASK NUMBER	
				5f. WORK UNIT NUMBER	
7. PERFORMING ORGANIZATION NAME(S) AND ADDRESS(ES) Carnegie Mellon University, Department of Material Science and Engineering ,5000 Forbes Avenue, Pittsburgh, PA, 15213				8. PERFORMING ORGANIZATION REPORT NUMBER	
9. SPONSORING/MONITORING AGENCY NAME(S) AND ADDRESS(ES)				10. SPONSOR/MONITOR'S ACRONYM(S)	
				11. SPONSOR/MONITOR'S REPORT NUMBER(S)	
12. DISTRIBUTION/AVAILABILITY STATEMENT Approved for public release; distribution unlimited					
13. SUPPLEMENTARY NOTES Proc. 1st Intl. Symp. on Metallurgical Modeling for Aluminum Alloys, Materials Solutions Conference 2003, Pittsburgh, (2003) pp. 163-168. U.S. Government or Federal Rights License					
14. ABSTRACT see report					
15. SUBJECT TERMS					
16. SECURITY CLASSIFICATION OF:			17. LIMITATION OF ABSTRACT Same as Report (SAR)	18. NUMBER OF PAGES 6	19a. NAME OF RESPONSIBLE PERSON
a. REPORT unclassified	b. ABSTRACT unclassified	c. THIS PAGE unclassified			

shapes in the aluminum sample, we need only specify a spatially homogeneous distribution of ellipsoids, $f(a, b, c)$, as the probability density of finding a grain that can be represented as an ellipsoid with semi-axis lengths a , b , and c aligned with a fixed sample coordinate system. Though a single orientation map is incapable of providing full information about $f(a, b, c)$. The full form of probability distribution $f(a, b, c)$ can be obtained using the orientation maps of orthogonal cross section of the sample[1].

Geometry generation

Once the shape distribution $f(a, b, c)$ has been obtained the simulation domain is populated with a collection of overlapping ellipsoids by placing them randomly inside the selected model microstructure. This is achieved by selecting a site at random inside the bounding box as the center of the ellipsoid. Next step is to decide the lengths of the semi-axes of the ellipsoid using the distribution $f(a, b, c)$. Out of this large set of overlapping ellipsoids, a small subset of optimal ellipsoids is picked such that each volume element is contained within one and only one ellipsoid. The procedure for selecting optimal packing is done using “simulated annealing” [2]. The procedure described above provides a set of ellipsoids to represent the grains in the final microstructure; however, these ellipsoids overlap in certain areas and do not fill space at other locations.

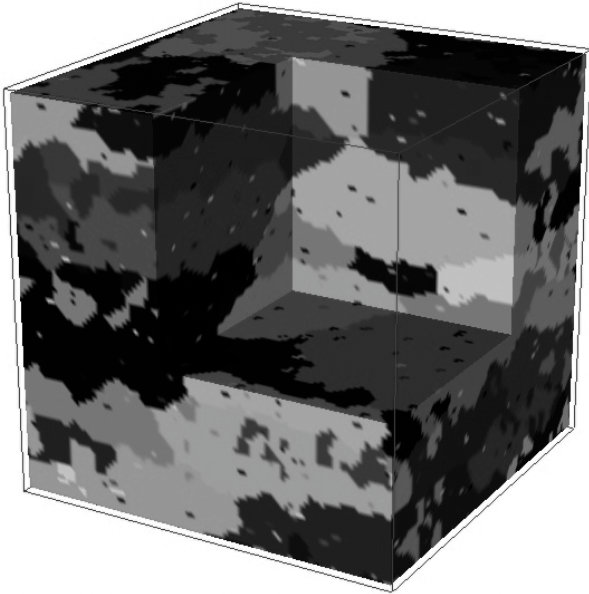


Figure2: Three dimensional geometry of the model microstructure. Grain shades were randomly assigned

The last step in generating the microstructure is to fill the space with grains that have the underlying ellipsoid distribution. First the space is sampled with a random sample of points. Then the space is tessellated using the Voronoi tessellation scheme [3]. The result of this scheme is a set of Voronoi cells. Each Voronoi cell is a volume enclosed by the perpendicular bisectors planes between adjacent points. Once this is completed the Voronoi cells grouped into grains. This is done by associating the cells with the ellipsoid containing it. If the cell lies in more than one ellipsoid it is associated with

the ellipsoid whose center is closest. This procedure ensures that a microstructure filling all the space and having no overlap is obtained. No overlap occurs since care is taken to assign the voronoi cells to one and only one grain.

Fig. 2 shows the typical three-dimensional microstructure generated based on the observations of the deformed aluminum 1050 alloy. On closer inspection one can see the coarser grains and also some smaller grains which are the nuclei introduced during the process of nucleation. Although aesthetic agreement between the model and the experimental observations is important, it is vital to compare the measured distributions of ellipsoids that served as the basis for the model to those obtained from the microstructure.

Microstructure Crystallography

The next step in the microstructure builder is the assignment of orientations to the grains in the model so as to match the microstructure of experimental aluminum polycrystal. Here the assumption is that the arrangement of grain orientations in a polycrystalline microstructure can be sufficiently characterized by specifying a combination of the distribution of grain orientations by volume fraction $f(g)$ and the distribution of relative misorientations across grain boundaries by area fraction $f(\Delta g)$. $f(g)$ and $f(\Delta g)$ are determined for the polycrystalline aluminum sample based on the geometric and crystallographic information from the orientation maps. For $f(g)$, this is accomplished by binning each orientation observation into the appropriate category of g . $f(\Delta g)$ is calculated in a similar fashion, except that, instead of counting the orientation observations, the misorientation associated with each pair of adjacent points that span a grain boundary is binned into the appropriate misorientation category.

After specifying $f(g)$ and $f(\Delta g)$, orientations are assigned to the grains in the model microstructure such that their distribution and arrangement matches both distributions using an iterative technique. The target $f(g)$ and $f(\Delta g)$ derived from the aluminum polycrystal, along with the topology data from the model microstructure, are the only pieces of information required for the orientation assignment algorithm. The algorithm is based on the work of Miodownik *et al.* [4] and uses a simulated annealing algorithm [2] to find an optimum configuration of orientations. Briefly, random orientations, g , are assigned to all of the grains in the model microstructure. Next, $f(g)$ and $f(\Delta g)$ are calculated and compared to their target values. An error value for the system (Φ) is calculated,

$$\Phi = \sum_i^{i_{\max}} \left[f^m(g)_i - f^e(g)_i \right]^2 + \sum_j^{j_{\max}} \left[f^m(\Delta g)_j - f^e(\Delta g)_j \right]^2 \quad (1)$$

where i sums over the orientation categories, j sums over the misorientation categories, and e and m signify experimental and model distributions, respectively. The algorithm proceeds by randomly choosing between two operations, an orientation change or an orientation swap, until the error value, Φ , is minimized.

Monte Carlo Simulation

Monte Carlo models are commonly used to describe grain growth and recrystallization [4-6]. In particular the Potts model was used in the simulations. The Potts model is flexible in terms of adjusting input parameters like energy and mobility and also it is computationally straightforward. The approach is briefly discussed here. Each lattice site in the microstructure, in from of a regular grid, generated by above described method, is given an index s_i based on the orientation. i.e. all the sites in the same grain have the same index (and also same orientation). The grain boundaries between different orientations have an excess energy, depending upon the misorientation between them, given by

$$E = \frac{1}{2} \sum_{i=1}^N \sum_{j=1}^n H(s_i, s_j) * [1 - \delta(s_i, s_j)] + F(s_i) \quad (2)$$

where the sums are over all the neighbor sites, n in total, of the site i and for all the N sites. For a pure isotropic grain growth $H(s_i, s_j) = E_0$, a constant, and for only curvature driven grain growth $F(s_i) = 0$.

New grains, or nuclei are introduced in to the microstructure at time, $t = 0$. The nucleation scheme used is discussed in detail in the next section.

Grain growth is carried out using Monte Carlo technique. It proceeds in the following way (i) lattice site is chosen at random (ii) a candidate index from the list of the neighboring indices is selected (iii) The change in system energy is calculated by using equation (2). (iv) The flip is performed with a probability $P(E)$ given by

$$P(E) = \begin{cases} p_0 & (E \leq 0) \\ p_0 \exp(-E/kT) & (E > 0) \end{cases} \quad (3)$$

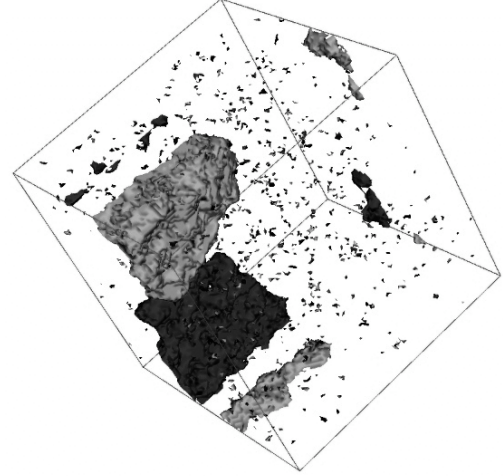
where

$$p_0 = \frac{M(g_i, g_j)}{M_m} \quad (4)$$

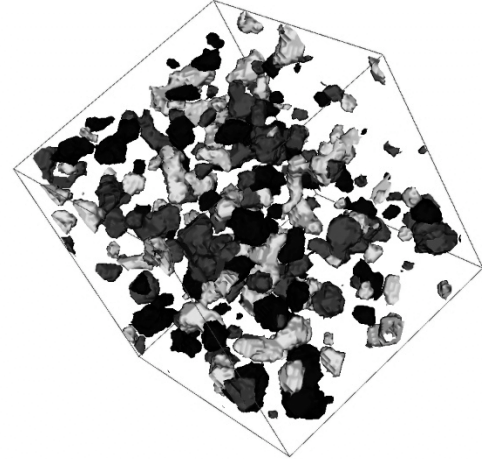
and $M(g_i, g_j) = \frac{1}{2}(m_{ij} + m_{ji})$ is the reduced mobility of that boundary between grains i and j where m_{ij} is the intrinsic mobility of that boundary and M_m is the maximum reduced mobility in the system. Thus an index flip is accepted with a probability proportional to the normalized boundary mobility.

Figure 3 shows a typical simulation result of recrystallization/grain growth simulation using the procedure described above. In Fig. 3(a) the original grain structure (coarser grains) is depicted along with the recrystallized nuclei introduced in the microstructure. By 1000 MCS, Fig. 3(b) the recrystallized nuclei are completely dominating. Recrystallization is almost completed at this point as the volume fraction of the recrystallized grains (sites) is about 0.95. In Fig. 3(c) it can be seen that the recrystallized grains are growing. Fig. 3(d) depicts a typical microstructure at the end of simulation. The simulation is stopped when the activity

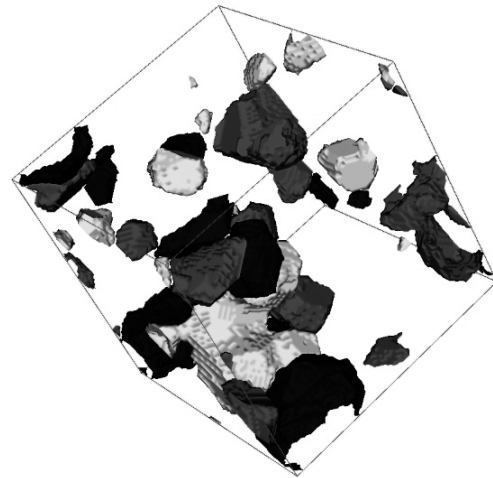
is very low or a predetermined number of MCS steps are performed.



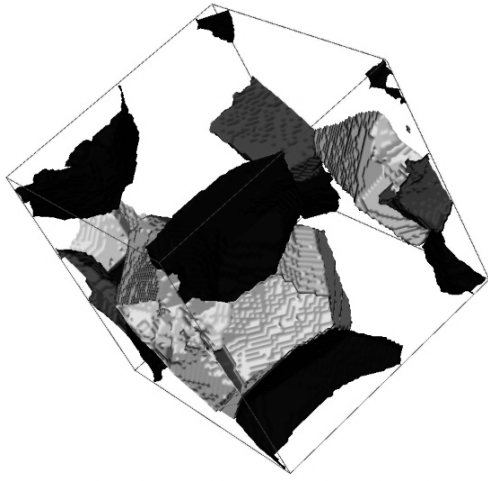
(a)



(b)



(c)



(d)

Figure 3 results of Monte Carlo simulation at (a) $t = 10$ MCS, (b) $t = 1000$ MCS, (c) $t = 10^4$ MCS and (d) $t = 10^5$ MCS. (Note: only a few grains have been selected for imaging in order to visualize the shapes of the growing grains. Also the lines seen on the grains in figure 3(d) are due to the discretization of the simulation domain)

Scaling of Monte Carlo simulation with experimental time can be carried out using various methods discussed in detail elsewhere [9]. The kinetics can be verified by the inspection of the plots of the average grain size against time, t (MCS).

Nucleation Scheme

The nucleation scheme being used in this work to introduce nuclei in the microstructure is outlined in Figure 4.

- 1) Select a site at random
- 2) Read its orientation information, x .
- 3) Get the probability of a new nucleus forming next to this texture $P(x)$.
- 4) Generate a random number R .
- 5) If $R < P(x)$ insert nucleus at the site.
- 6) Else reject
- 7) Keep doing this till we reach the volume fraction, predefined.

Figure 4: Algorithm for choosing a site for nucleation.

The orientation of these nuclei can either be random or the scheme depicted in figure 5 can be used.

- 1) Choose an orientation at random, x_1 .
- 2) Find probability of having a nucleus with texture x_1 next to grain with texture x , $P(x_1, x)$.
- 3) Generate a random number R_1
- 4) If $R_1 < P(x_1, x)$ accept this as the nucleus texture.
- 5) Else reject.

Figure 5: Algorithm for assigning orientation to the nucleus.

The algorithm in Fig. 4 is explained as follows. Assume a site is chosen in the microstructure and the orientation around this site is computed. Assume that the dominant texture around the site is cube. Now the probability of that a new nucleus being next to cube texture is computed e.g. 0.10. Random number between 0 and 1 is then generated. If this random number is less than 0.10 then the move to put the new nucleus at the chosen site is accepted. Otherwise another site is picked from the microstructure and steps 2 through 6 from Figure 4 are repeated.

Similarly to choose the orientation for a nucleus, algorithm as shown in Fig. 5 may be employed. First the texture around the nucleus is determined, e.g. cube. Choose a random orientation for this nucleus, e.g. Goss. Then the probability of the nucleus having Goss texture sitting next to a cube texture is determined according to an appropriate rule, e.g. 0.05. Now generate a random number. If this random number is less than 0.05 the move to use Goss as the texture for the nucleus is accepted, else steps 1 through 5 in Figure 5 are repeated.

The microstructure used in the simulations was similar to the one depicted in Figure 2, having pancake shaped grains with the aspect ratio for the semi-axes being 1:1:0.2. A substantial fraction of the deformation texture did not correspond to one of the standard texture components commonly used for texture analysis in FCC metals. For the purposes of this paper, this part of the texture is referred to as the ‘undefined components’ whose center of gravity is approximately (90, 0, 15) and (35, 0, 5) in Euler angles. The dependence of microstructural evolution on probability of insertion of nuclei next to the “undefined” texture is investigated in the simulations. Three independent simulations were carried out by changing the probability, P , of insertion of nuclei next to the “undefined” texture. In these simulations the total volume fraction of nuclei is held constant at 0.02. Each nucleus inserted in the microstructure consists of 3 voxels. At the start of the simulations the number of grains in the system is approximately 6700. Only the simulation results up to the point where the number of grains in the system is more than 50 need to be considered from a statistically perspective. In the three simulations discussed, the probability P , discussed earlier, is varied from 0 to 0.2 to 0.5.

Results

Table 1 shows the fractions of the various texture components at the start of simulations (including nuclei). See a standard text on texture for definitions of the components, e.g. [Kocks, U.F., C. Tomé, and H.-R. Wenk, eds. Texture and Anisotropy. 1998, Cambridge University Press, Cambridge, UK.]. It can be seen that the values for the volume fractions of the texture components are comparable across the table. For example, the volume fraction of the cube component is almost same in all the three simulation runs.

Table 1 Fractions of the various texture components at the start of simulation.

Probability	Cube	Brass	Goss	Dilla-more	Coppe r	S	Cube Rotate d
0	0.024	0.065	0.045	0.025	0.049	0.285	0.043
20	0.025	0.064	0.043	0.025	0.048	0.294	0.047
50	0.025	0.063	0.042	0.026	0.047	0.298	0.046

Figure 6 shows a plot of the number of grains in the simulations as a function of time in units of MCS. It can be seen that the evolution, in all the three cases, in terms of number of grains is very similar. With the number of grains at the start of the simulations was about 6700 grains and at the end each of them had between 100 and 50 grains. Also a peak and turn-around 1000 MCS, Fig. 6 is the point at which the recrystallization is complete and at which grain growth starts. The results of these three simulations are presented in Figures 7, 8 and 9.

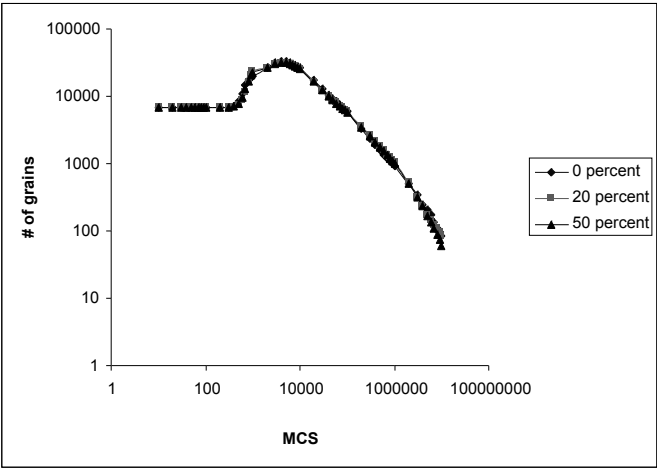


Figure 6: Plot of number grains against time (MCS).

The figure 7 shows the evolution of the various texture components for the value P 0. It can be seen that the simulation starts with a strong S component. At the end of the simulation none of the standard texture component dominates but the volume fraction of cube component is the highest at 0.05.

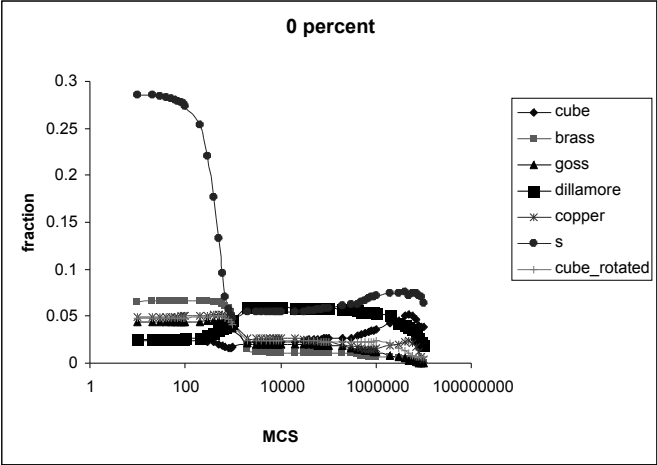


Figure 7: Evolution of the various components as a function of time when probability, P, is 0.

Figure 8 shows the evolution of the various texture components at probability at 0.20. At the end of the

simulations the percentage of cube is a slightly higher at 0.084.

Figure 9 shows similar plot for P = 0.50. Towards the end of the simulations the cube texture becomes the dominant component. The value for the cube component is the highest at 0.243.

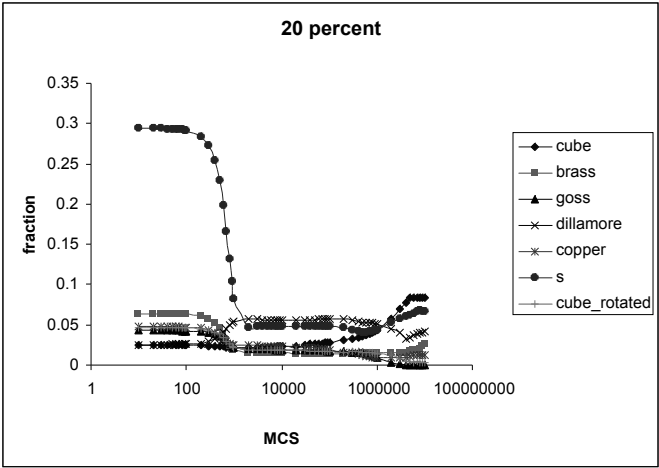


Figure 8: Evolution of the various components as a function of time when probability, P, is 0.20.

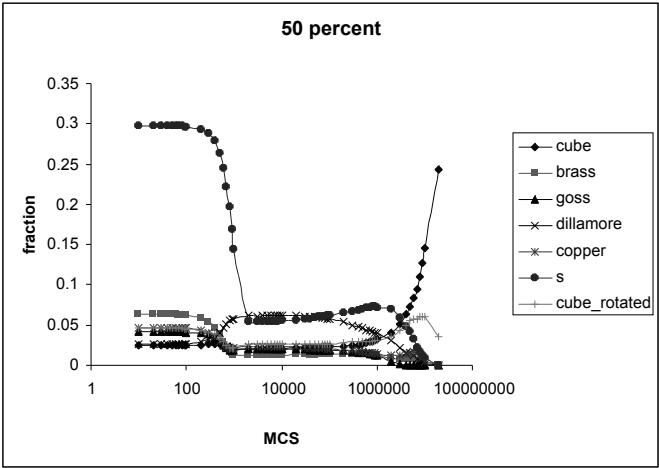


Figure 9: Evolution of the various components as a function of time when probability, P, is 0.5.

Table 2. Change in the volume fraction of cube as we change the probability of nuclei occurring next to the “undefined” texture

Probability(P) %	Volume fraction of cube
0	0.05
20	0.085
50	0.243

Conclusions and Future work

Preliminary results indicate that nucleation scheme has a strong impact on the evolution of microstructure (Table 2). There is a clear indication that the change in the volume fraction of cube at the end of simulations with different starting conditions depends on the probability rule. Further simulations are planned to investigate the effects of other input parameters on microstructure evolution like relative volume fraction of other components. Also

planned are simulations for recrystallization and calibration of grain size distributions and kinetics against the experimental data.

Acknowledgement

This work is supported in part by the Programming, Environment and Training program, US DoD, and in part by the MRSEC program of the National Science Foundation under Award Number DMR-0079996.

References

1. Saylor D. M., Fridy J., El-Dasher B. S., Jung K. H., and Rollett A. D., "Statistically Representative Three-Dimensional Microstructures Based on Orthogonal Observation Sections" Metallurgical and Materials Transactions, submitted 2003
2. Press W. H., Vetterling W. T., Teukolsky S. A., and Flannery B. P.: *Numerical Recipes in C++: The Art of Scientific Computing* Second Edition, Cambridge University Press, New York, 2002, pp. 448-455.
3. Møller J.: *Lectures on Random Voronoi Tessellations: Lecture Notes in Statistics* v. 87, Springer-Verlag, New York, 1992
4. Miodownik M., Godfrey A. W., Holm E. A., and Hughes D. A.: *Acta. Mater.* 1999, vol. 47, 2661-2668
5. Anderson M. P., Grest G. S., Srolovitz D. J.: *Phil. Mag. B* 1989; 59:293.
6. Hassold G. N., Holm E. A.: *Computers in Physics* 1993; 7:97.
7. Holm E. A., Hassold G. N., Miodownik M. A.: *Acta. Mater* 2001; 49:2981.
8. Wu F. Y.: *Rev. Mod. Phys.* 1982 vol. 54[1] 235-268.
9. Raabe D.: *Acta. Mater.* 2000, vol. 48 1617-1628